

# Aberrant Synaptic Transmission in the Hippocampal CA3 Region and Cognitive Deterioration in Protein-Repair Enzyme-Deficient Mice

Yuji Ikegaya,<sup>1</sup> Mitsunori Yamada,<sup>2</sup>  
Tetsuya Fukuda,<sup>3</sup> Hidehito Kuroyanagi,<sup>4</sup>  
Takuji Shirasawa,<sup>4,5</sup> and Nobuyoshi Nishiyama,<sup>1,5\*</sup>

<sup>1</sup>Laboratory of Chemical Pharmacology, Graduate School of Pharmaceutical Sciences, University of Tokyo, Tokyo, Japan

<sup>2</sup>Department of Pathology, Brain Research Institute, Niigata University, Niigata, Japan

<sup>3</sup>Department of Anatomy, School of Medicine, Keio University, Tokyo, Japan

<sup>4</sup>Department of Molecular Genetics, Tokyo Metropolitan Institute of Gerontology, Tokyo, Japan

<sup>5</sup>CREST, Japan Science and Technology Corporation, Tokyo, Japan

**ABSTRACT:** L-aspartate is the amino-acid residue most susceptible to spontaneous isomerization. This denaturation causes an alteration in the biological activity of the protein and is regarded as an aging process of the protein. Protein L-isoaspartyl methyltransferase (PIMT) repairs this post-translational modification and thus is implicated in retarding the aging process of proteins. PIMT is highly expressed in the brain, and its deficiency results in progressive epilepsy after 4 weeks of age, with a fatal seizure in mice. Here we report the pathophysiological role of this repair system in the hippocampal slice of PIMT-deficient mice. The hippocampal mossy fiber-CA3 synapses of PIMT-deficient mice showed hyperexcitation that was repressed by a  $\gamma$ -aminobutyric acid (GABA)<sub>A</sub> receptor agonist muscimol. In addition, the mossy fiber-CA3 synapses failed to show long-term potentiation or paired-pulse facilitation. No abnormality, however, was observed in Schaffer collateral-CA1 synapses or in perforant path-dentate gyrus synapses. Electron microscopic study revealed aberrant distribution of synaptic vesicles in the mossy fiber terminals and vacuolar degeneration at the axon hillock of dentate granule cells in PIMT-deficient mice. Furthermore, the PIMT-deficient mice showed impaired spatial memory in Morris water maze test and exhibited fewer anxiety-related behaviors in the elevated-plus test. These results suggest that the mossy fiber-CA3 system is vulnerable to aspartate isomerization and that the PIMT-mediated repair system is essential for maintenance of

normal functions of the hippocampus. *Hippocampus* 2001;11:287–298. © 2001 Wiley-Liss, Inc.

**KEY WORDS:** protein L-isoaspartyl methyltransferase; mossy fiber; long-term potentiation; learning and memory; epilepsy

## INTRODUCTION

L-asparaginyl and L-aspartyl residues are a prime subject to spontaneous degradation reactions that yield isomerized and racemized aspartyl derivatives in aged proteins (Geiger and Clarke, 1987; Stephenson and Clarke, 1989). Proteins carrying L-isoaspartyl and D-aspartyl residues change their structures, and their biological activities are decreased. These modified residues are recognized by a highly conserved cytosolic enzyme, protein L-isoaspartyl methyltransferase (PIMT) (Clarke, 1985). Enzymatic methylation of these altered residues is an indispensable step for a reversion to normal L-aspartyl residues (Johnson et al., 1987; McFadden and Clarke, 1987; Ladino and O'Connor, 1992; Lindquist and McFadden, 1994; Galletti et al., 1995). PIMT is thus suggested to repair and prevent the accumulation of poten-

Grant sponsor: CREST, Japan Science and Technology Corporation. Present address of H.K. is Department of Anatomy, Jichi Medical School, Tochigi 329-0498, Japan.  
\*Correspondence to: Dr. Nobuyoshi Nishiyama, 7-3-1 Hongo, Bunkyo-ku, Tokyo 113-0033, Japan. E-mail: nisiyama@mol.f.u-tokyo.ac.jp  
Accepted for publication 6 December 2000

tially dysfunctional proteins. In this context, this repair system is supposed to hinder the aging process at the cellular and tissue level and function as an antisenesescence device.

Although enzymatic activity is detectable in all vertebrate tissues, extremely high PIMT activity is present in the brain (Johnson et al., 1991). We and others generated PIMT-deficient mice by targeted disruption of the PIMT gene (Kim et al., 1997; Yamamoto et al., 1998). Those mice over age 4 weeks unexpectedly displayed progressive epilepsy with diverse types of ictal seizures, including myoclonic jerk, forelimb clonus, and grand mal attack, and eventually succumbed to a fatal paroxysm at an average of 6 weeks. Because the brain of 6-week-old PIMT-deficient mouse showed no sign of aging, these results strongly suggest an alternative role of PIMT in addition to an anti-aging function.

The limbic system, particularly the hippocampal formation, is involved in certain types of epilepsy (Schwartzkroin, 1994). Indeed, temporal lobe epilepsy often results in hippocampal sclerosis. In the present study, using electrophysiological and histochemical techniques, we evaluated the hippocampus of PIMT-deficient mice in order to elucidate the pathogenic mechanism of aspartate isomerization. Here we show the physiological and morphological abnormalities in the mossy fiber-CA3 synapses of PIMT-deficient mice. These findings indicate that the repair of an isomerized aspartate residue is essential for normal functioning of the central nervous system, particularly in the hippocampal mossy fiber system. Furthermore, learning and emotional impairment was observed in PIMT-deficient mouse. Thus the mossy fibers are not only vulnerable to protein aging due to aspartate isomerization, but also play a pivotal role in cognition and emotion.

## MATERIALS AND METHODS

### Animals

A PIMT knockout mouse was prepared as previously described (Yamamoto et al., 1998), having been backcrossed for 4–5 generations (N4–N5) to the inbred C57BL/6J strain of mice. The animal was kept under temperature- and humidity-controlled conditions ( $22 \pm 1^\circ\text{C}$ ,  $55 \pm 10\%$ , respectively) and was housed individually in a plastic cage. The mouse had free access to food and water. All efforts were made for the care and use of animals according to the NIH Guide for the Care and Use of Laboratory Animals.

### Electrophysiology

A mouse was decapitated and the brain was quickly removed. The hippocampus was cut into 300- $\mu\text{m}$ -thick slices in ice-cold artificial cerebrospinal fluid (ACSF), and the slices were then submerged in ACSF at  $32^\circ\text{C}$  for  $>1$  h. The stratum granulosum was stimulated with a bipolar electrode, and the evoked potential was extracellularly recorded from the stratum lucidum with a glass capillary microelectrode filled with 0.15 M NaCl. In some experiments, field potential evoked by stimulation of the Schaffer col-

laterals and the perforant paths was recorded from the CA1 stratum radiatum and the dentate molecular layer, respectively. Test stimulation (100  $\mu\text{s}$  duration) was applied at intervals of 30 s, and its stimulus intensity was adjusted in the range of 100–400  $\mu\text{A}$  so that it produced about 50% of the maximal amplitude of field excitatory postsynaptic potential (fEPSP). To induce long-term potentiation (LTP), at  $>30$  min after the response became stable, a tetanic stimulation (twice 100 Hz for 1 s at an interval of 30 s) was applied to the mossy fibers or the Schaffer collaterals through the same electrode used for the test stimulation. Potentiation of evoked potentials following tetanic stimulation was evaluated by measuring changes in fEPSP slope. The fEPSP slope was defined as the maximal slope in a rise phase of the negative field potential via a computational analysis (Wave-kun, Tokyo, Japan) of the analog-to-digital converted signals. ACSF was composed of 127 mM NaCl, 1.6 mM KCl, 2.4 mM  $\text{CaCl}_2$ , 2.4 mM  $\text{MgSO}_4$ , 1.3 mM  $\text{KH}_2\text{PO}_4$ , 1.24 mM  $\text{NaHCO}_3$ , and 10.0 mM glucose, and was saturated with 95%  $\text{O}_2$ -5%  $\text{CO}_2$ .

### Timm Staining

The removed brain was quickly frozen at  $-15^\circ\text{C}$  and was coronally cut at 14- $\mu\text{m}$  thickness with a cryostat (Cryocut 1800, Fine-tec Scientific Instruments Co., Ltd., Tokyo, Japan). For Timm stain, the sections were washed with 0.1 M phosphate buffer (PB) and were then immersed in 0.37% sodium sulfide solution for 10 min, immediately followed by fixation with 10% (v/v) formaldehyde solution for 15 min. After being washed with 0.1 M PB, the sections were dehydrated with 70% and 96% ethanol, and dried. To perform sulfide silver staining, they were incubated with the physical developer, citrate-buffered 20% Arabic gum solution containing 1.7%  $\text{AgNO}_3$  and 0.085% hydroquinone, in a dark room at  $26^\circ\text{C}$  for 50 min. The slices were washed with distilled water at the end of the reaction. As a counter stain, Nissl stain was performed with 0.1% cresyl fast violet.

### Immunohistochemical Analysis

Mice were perfused transcardially with 0.02 M phosphate-buffered saline (PBS), followed by ice-cold 10% formalin containing 0.5% glutaraldehyde in 0.1M PB. Their heads were cut off, and immersed in the same fixative overnight at  $4^\circ\text{C}$ . After dehydration through an ascending ethanol series, the brains were embedded in paraffin, and cut serially at 5- $\mu\text{m}$  thickness on a rotary microtome (HM-325, Microm, Heidelberg, Germany). After deparaffinization, some sections were used for Nissl staining, and others were processed for immunohistochemistry. The antibodies used in this study were as follows: rabbit antiserum against neurofilament (NF) (Fukuda et al., 1997; generous gift from Dr. Y. Takahashi, Niigata University, Niigata, Japan, 1:5,000 dilution), monoclonal antibody against microtubule-associated protein (MAP)-2 (Boehringer Mannheim, 1:50), and mouse monoclonal antibody against growth-associated protein B-50 (GAP-43) (Mercken et al., 1992; Innogenetics, Zwijndrecht, Belgium, 1:100). In order to examine the GABAergic system in PIMT-deficient mice, antiserum against gamma aminobutyric acid (GABA) (Carlton and Hayes, 1990; Chemicon, Temecula, CA, 1:1,000) or a GABA-synthesizing en-

zyme, glutamic acid decarboxylase (GAD)-65/67 (Erlander et al., 1991; Affinity Research Products, Mamhead Castle, UK, 1:1,000), was also used. For analysis of the mossy fiber system in PIMT-deficient mice, we also used mouse monoclonal antibody against highly polysialylated neural cell adhesion molecule (PSA-NCAM) (Seki and Arai, 1991; supplied by Dr. T. Seki, Juntendo University, Tokyo, Japan, 1:200), which is one of the neural cell adhesion molecules and was previously demonstrated to be expressed on the mossy fibers as well as dentate granule cells in the adult hippocampus (Seki and Arai, 1993). Sections were incubated overnight at 4°C with the primary antibodies diluted with 0.02 M PBS containing 0.5% skim milk, and then incubated with secondary antibodies for 1 h at 37°C. As secondary antibodies, peroxidase-labeled anti-rabbit IgG (Medical and Biological Laboratories, Nagoya, Japan, 1:100) was used for anti-NF, anti-GABA, and anti-GAD-65/67, and peroxidase-labeled anti-mouse IgG (Medical and Biological Laboratories, 1:100) was used for anti-MAP-2 and anti-GAP-43. In case of anti-PSA-NCAM, the avidin-biotin-peroxidase complex (ABC) method was used, because this antibody was mouse IgM. After incubation with the primary antibodies, sections were treated with biotinylated anti-mouse IgM (Vector, Burlingame, CA, 1:100) at 37°C for 30 min and then incubated with ABC solution (Vector) at 37°C for 30 min. All these immunoreactions were visualized in 0.05 M Tris buffer, pH 7.4, containing 0.01% diaminobenzidine tetrahydrochloride (DAB) and 0.01% hydrogen peroxide at 37°C for 5–15 min.

### Electron Microscopic Study

For an electron microscopic examination, mice were anesthetized by inhalation of ether, and perfused transcardially with PBS followed by 3% glutaraldehyde and 1% paraformaldehyde in 0.1 M PB (pH 7.4). The brains were removed from the crania and immersed in the same fixative at 4°C for 48 h. The cerebra were cut coronally and then the hippocampal CA3 regions and dentate gyri were dissected out. Tissue blocks were postfixed in 1% osmium tetroxide, dehydrated in a graded ethanol series, and embedded in Epon 812. Ultrathin sections from PIMT-deficient or control mice were stained with uranyl acetate and lead citrate, and examined with a Hitachi H-7100 electron microscope.

### Locomotor Activity Test

Five minutes after a mouse was placed in the doughnut-shaped apparatus (320-mm outer diameter, 160-mm inner diameter, 130-mm wall height) (AT-320, Toyo Sangyo Co., Ltd., Toyama, Japan), the numbers of horizontal movement actions, turning actions or rearing actions, total movement time, total movement distance, and average speed were automatically monitored for 30 min with 144 infrared sensors at scanning rate of 10 Hz. The sensors placed 65 mm in height from the cage bottom detected rearing actions.

### Water Maze Test

A modified water maze (Morris, 1984) was used to assess visuospatial learning and memory performance. A circular tank

(680-mm diameter) was filled with 18–19°C water to a depth of 270 mm. The pool was illuminated by room lights, and all visual cues around the room were kept constant from day to day. Four points on the perimeter of the pool were designated north (N), east (E), south (S), and west (W), thus dividing the pool into four quadrants (NW, NE, SE, and SW). On the day before the test, the mouse was placed in the pool for 60 s in order to habituate it to the training environment. On the first day (day 0), the 100-mm-diameter black platform, onto which the mouse could escape, was positioned 5 mm over the water surface and in the center of the quadrant SW, and animals were immersed into point E of the pool. On trial test days (day 1–5), a transparent platform was positioned 5 mm below the water level in the same quadrant SW, and the mouse was trained for four trials a day. The immersion points varied between N, S, E, and W in a quasirandom order for each day so that the mouse would not be able to predict the platform location from the point at which it was placed in the pool. On mounting the platform, the mouse was given a 60-s period. If a mouse failed to find the platform within 90 s, it was manually forced to be on the platform for 60 s. Latency from the immersion into the pool to the escape onto the platform (escape latency) was automatically recorded for each trial by a behavior tracing analyzer (BTA-2A, Muromachi Kikai Co., Ltd., Tokyo, Japan). On day 6, the platform was removed from the pool, and each mouse was placed at point E and was allowed 90 s of free swimming (probe trial). The total duration that the mouse swam in the quadrant NE, NW, SE, or SW was recorded. If a spontaneous seizure occurred during testing, the mouse was allowed a 60-min rest before resuming to the testing.

### Spontaneous Alternation Behavior Test

The behavior experiment was conducted in a Y-shaped maze. The three trough-shaped arms (395 mm in length, 120 mm in height) were separated by angles of 120°. A mouse was placed in one arm of the apparatus and was allowed to explore the maze for a period of 8 min. Arm choices were manually recorded during this time. Any three consecutive choices of three different arms were counted as an alternation. The percentage of alternation was determined by dividing the total number of alternations by the total number of choices minus 2. The memory component in this task is that the mouse must remember which arm was more recently visited in order to alternate.

### Step-Through Test

The apparatus (PA M1, O'Hara and Co., Ltd., Tokyo, Japan) consists of two compartments separated by a black wall with a hole in the lower middle part so that a mouse can go through the wall. A fluorescent light illuminated one chamber, and the other was dark with opacity walls. The test was performed on 2 consecutive days at the same time of day. In the learning trial (day 1), the mouse was placed in the bright compartment. Immediately after stepping into the dark compartment, the animal received an electric shock to its paws (36 V, AC) through a stainless-steel grid floor. The time until the mouse entered the dark chamber (latency) was recorded. In the test trial (day 1), the same test procedure was followed and latency was measured, with a ceiling score of 300 s.

## Elevated-Plus Maze Test

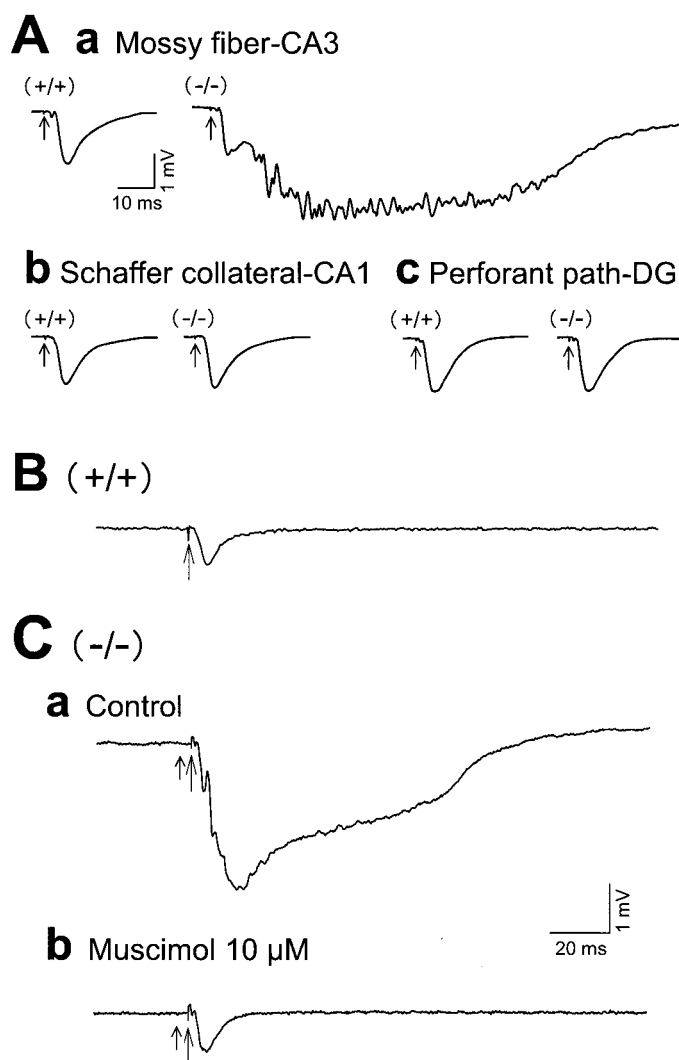
The apparatus was constructed of black-painted plastic panels and was arranged as a cross with two open arms facing each other. The other two arms were enclosed by a 248-mm-high wall. The arms measured  $80 \times 248$  mm and were raised by a single central support to a height of 253 mm above the floor. The four arms extended from a common central platform ( $80 \times 80$  mm). The mouse was placed on the deepest portion of the closed arm and allowed to explore the maze for 3 min. Behavior on the maze was recorded with a BTA-2A tracing analyzer (Muromachi Kikai), and the percentage of time spent on the open arms was calculated.

## RESULTS

### Abnormal Neurotransmission at Mossy Fiber Synapse in PIMT-Deficient Mice

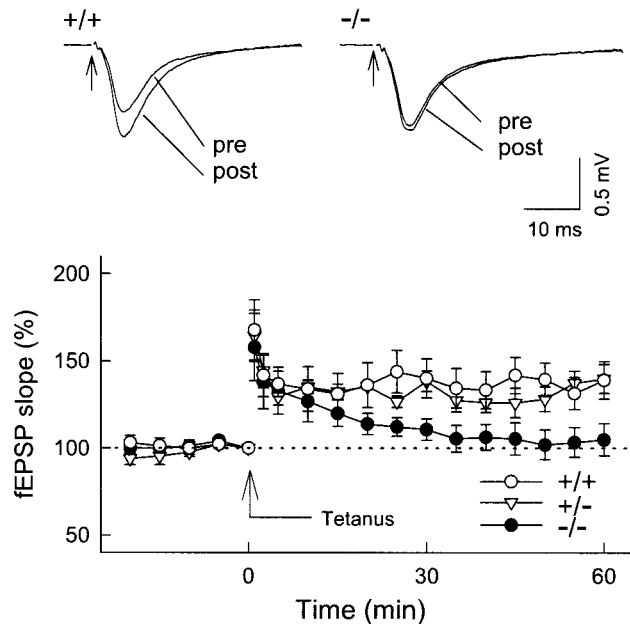
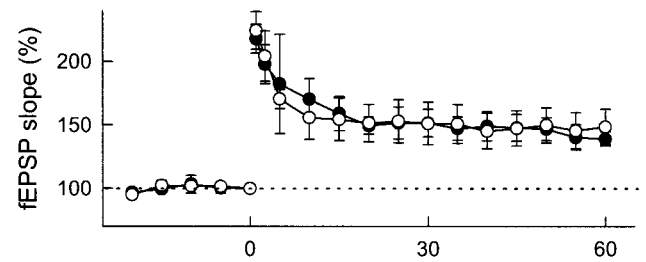
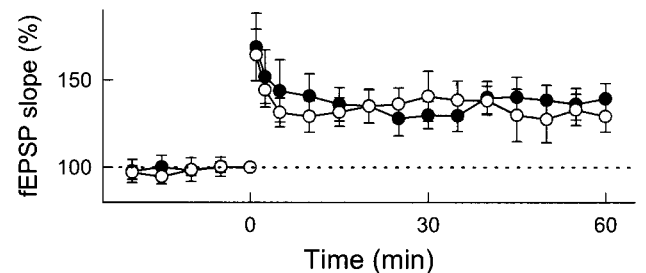
Since we previously found that PIMT-deficient mice show fatal progressive epilepsy after 4 weeks of age (Yamamoto et al., 1998), neurotransmission in hippocampal slices prepared from 5-week-old mice was evaluated by extracellular recording of field potentials. Upon stimulation of mossy fibers, an aberrant field response was recorded from the CA3 stratum lucidum in 20 out of 31 PIMT $^{-/-}$  slices (Fig. 1Aa, Ca). In these cases, the duration of field potentials was extensively prolonged; duration was in the range of 100–200 ms, while that in the wild-type hippocampal slice was 7–12 ms (Fig. 1B). The aberrant field potential was completely blocked by either the voltage-sensitive Na<sup>+</sup> channel tetrodotoxin or the non-N-methyl-D-aspartate receptor antagonist CNQX. Therefore, the abnormal field response was apparently produced by synaptic activities. In addition, because the abnormal fEPSP recovered to a normal level after an application of 10  $\mu$ M muscimol, a  $\gamma$ -aminobutyric acid (GABA)<sub>A</sub> receptor agonist (Fig. 1Cb), the prolonged response was likely a result of reduced activity of GABAergic neurons. Three of 11 slices prepared from PIMT $+/+$  mice also showed prolonged fEPSP. However, no abnormal synaptic transmission was observed in the slices prepared from 3-week-old PIMT-deficient mice that were symptomatically free from epilepsy (data not shown). By contrast, the Schaffer collaterals-CA1 or the perforant path-dentate gyrus synapses showed no aberrant response in PIMT $^{-/-}$  or PIMT $+/+$  mice (Fig. 1Ab, Ac). Taken together, the mossy fiber-CA3 neurotransmission was selectively altered among the hippocampal trisynaptic pathways, and the mossy fiber malfunction may be involved in the etiology of progressive epilepsy of PIMT-deficient mice.

We next examined whether long-term potentiation (LTP), a type of synaptic plasticity that may underlie learning and memory (Bliss and Collingridge, 1993; Izquierdo and Medina, 1995; Martinez and Derrick, 1996), was affected in PIMT-deficient mice. Because LTP may be inappropriately assessed when the fEPSP with extraordinarily prolonged duration was included in the data, the slice showing normal fEPSP duration was employed in the following experiments. Hippocampal slices were prepared from



**FIGURE 1.** Representative field potentials in hippocampal slice prepared from 5-week-old PIMT $+/+$  (+/+) or PIMT $^{-/-}$  mouse ( $-/-$ ). **A:** Field potentials evoked by stimulation of mossy fibers, Schaffer collaterals, and perforant path were recorded from CA3 stratum lucidum (a), CA1 stratum radiatum (b), and dentate molecular layer (c). **B, C:** Field potentials evoked by stimulation of dentate gyrus were recorded from CA3 stratum lucidum of 5-week-old PIMT $+/+$  (B) or PIMT $^{-/-}$  mouse (C). PIMT $^{-/-}$  slice showed a massive and prolonged negative field potential of the mossy fibers (Aa, Ca), and the abnormal response was alleviated by an application of muscimol 10  $\mu$ M (Cb). Stimulation was applied at times indicated by arrows. DG, dentate gyrus.

5-week-old mice. The baseline fEPSP before LTP induction was not uniform: fEPSP slope was  $1.50 \pm 0.24$  V/s in PIMT $+/+$  mice (mean  $\pm$  SEM of  $N = 7$ ),  $1.26 \pm 0.24$  V/s in PIMT $+/+$  mice ( $N = 7$ ), and  $2.38 \pm 0.42$  V/s in PIMT $^{-/-}$  mice ( $N = 8$ ). Thus, the fEPSP slope in PIMT $^{-/-}$  mice was significantly enhanced (analysis of variance (ANOVA):  $F(2,21) = 5.29$ ,  $P = 0.01$ ; Tukey's test:  $Q(3,21) = 4.28$ ,  $P < 0.05$  between PIMT $+/+$  and PIMT $^{-/-}$  mice). When tetanic stimulation was applied to the mossy fibers, LTP was induced in both PIMT $+/+$  and PIMT $+/+$  mice. However, LTP was not induced by tetanic stim-

**A** Mossy fiber-CA3 (5 wk old)**B** Schaffer collateral-CA1 (5 wk old)**C** Mossy fiber-CA3 (3 wk old)

**FIGURE 2.** Long-term potentiation in mossy fiber-CA3 synapse (A, C) and Schaffer collateral-CA1 synapse (B). **A:** Upper traces represent typical mossy fiber responses recorded from 5-week-old PIMT+/+ slice (left) or PIMT-/- slice (right) immediately before (pre) and 60 min after (post) tetanic stimulation. Arrows indicate time of test stimulation. Lower graph shows time course of fEPSP slope following tetanic stimulation, which was applied at the time 0 (Tetanus). fEPSP slope is expressed as a percentage of baseline value immediately before tetanic stimulation. Data are means  $\pm$  SEM of 7–9 cases.

mediately before tetanic stimulation. In PIMT+/+ mouse (open circles) and PIMT+/- mouse (open triangles), robust LTP was induced, but no LTP was generated in PIMT-/- mouse (solid circles). **B:** Schaffer collateral-CA1 LTP was normal in 5-week-old knockout mouse. Symbols are the same as those in A. **C:** PIMT-/- slice displays normal mossy fiber-CA3 LTP at 3 weeks of age, when the mouse has not developed epilepsy. Data are means  $\pm$  SEM of 7–9 cases.

ulation in PIMT-/- mice, while short-term potentiation was normally generated (fEPSP slopes at time of 60 min: ANOVA:  $F(2,25) = 4.38$ ,  $P = 0.02$ ; Tukey's test:  $Q(3,25) = 3.60$ ,  $P < 0.05$  between PIMT+/+ and PIMT-/- mice) (Fig. 2A). Incidentally, the slice with a long-duration fEPSP also failed to show LTP ( $N = 4$ , data not shown). As for the Schaffer collateral-CA1 synapse in PIMT-deficient mice, baseline fEPSP was similar to that of wild-type mice, and LTP was normally induced (Fig. 2B) (Student's  $t$ -test:  $t(12) = 0.63$ ,  $P = 0.54$ ). The PIMT-deficient mice during the latent period of epilepsy also showed a robust CA3 LTP (Fig. 2C) (Student's  $t$ -test:  $t(12) = 0.81$ ,  $P = 0.43$ ).

In order to clarify the presynaptic contribution to altered neurotransmission, the paired-pulse responses of mossy fiber synapses were investigated in 5-week-old mice. Paired-pulse synaptic plasticity is generated predominantly by presynaptic alteration (Zucker, 1989). Paired-pulse facilitation was induced at 20–80-ms interpulse intervals in PIMT+/+ and PIMT+/- mice. Paired-pulse depression, on the contrary, was evoked at interpulse intervals of 20–1,000 ms in PIMT-deficient mice (Fig. 3) (two-way ANOVA:  $F(2,120) = 97.61$ ,  $P < 0.001$ ; Tukey's test:  $Q(3,120) = 17.35$ ,  $P < 0.01$  between PIMT+/+ and PIMT-/- mice). These results suggest that the alternation in presynaptic function of mossy fiber synapses may account for the abnormal hippocampal physiology in PIMT-deficient mice.

### Histological Abnormalities in the Hippocampus of PIMT-Deficient Mice

Hippocampal sections prepared from 6-week-old PIMT-deficient mice showing the symptom of epileptic seizures were stained with the Timm method, a histochemical technique labeling synaptic terminals of the mossy fibers (Danscher and Zimmer, 1978). Epileptic patients as well as experimental epileptic animals are often associated with ectopic sprouting of mossy fibers into the dentate molecular layer and the stratum oriens (Tauck and Nadler, 1985; Sutula et al., 1988; Babb et al., 1991; Van der Zee et al., 1995; Ikegaya, 1999; Ikegaya et al., 2000). However, our epileptic mice did not display the mossy fiber sprouting (Fig. 4A–F). We next investigated the localization of the immunoreactivity for PSA-NCAM in the hippocampus of PIMT-deficient mice. PSA-NCAM immunoreactivity was evident throughout the stratum lucidum of PIMT-deficient mice (Fig. 4H), while faint immunostaining was detected in the same region of control mice (Fig. 4G). Likewise, despite the subtle immunoreactivities of PSA-NCAM in the dentate gyrus of wild mice (Fig. 4I), we observed that PSA-NCAM-positive processes perforated perpendicularly through the stratum granulosum of PIMT-deficient mice (Fig. 4J). These abnormal projections were not detected in 3-week-old PIMT-deficient mice. Furthermore, no alterations were observed in immu-

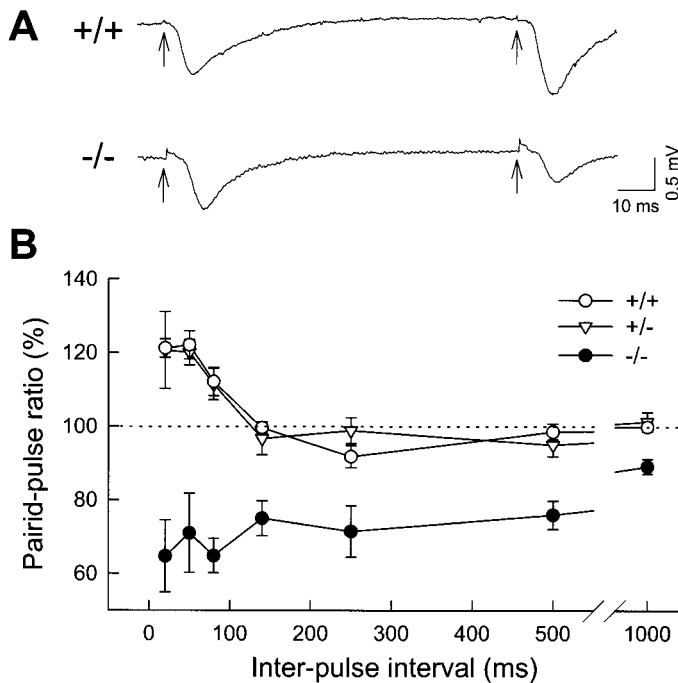


**FIGURE 3.** Paired-pulse modulation of mossy fiber-CA3 synapse of 5-week-old mouse. **A:** Archetypal paired-pulse responses recorded from PIMT+/+ slice (upper) or PIMT-/- slice (lower). Mossy fibers were stimulated at times indicated by arrows. **B:** Paired-pulse ratios are expressed as ratios of second response to first response. PIMT-/- slice (solid circles) demonstrated paired-pulse depression, although PIMT+/+ slice (open circles) and PIMT+/- slice (open triangles) showed an increase in paired-pulse ratio when the paired-pulse interval was less than 140 ms. Data represent mean  $\pm$  SEM of 7–8 cases.

nohistochemical staining for GAD-65/67, GABA, GAP-43, MAP-2, or NF in the hippocampus of 5-week-old PIMT-deficient mice (data not shown).

We next investigated the ultrastructure of mossy fibers and somatic structures of dentate granule cells by using electron microscopy. In the hippocampal CA3 region of PIMT-deficient mice, widespread degeneration was found in mossy fiber terminals. Synaptic vesicles of round type in the presynaptic regions of mossy terminals were aberrantly distributed, i.e., vesicles were located more centrally than peripherally in the presynaptic terminals (Fig. 5A,B). Various-sized aggregates of synaptic vesicle were near the synaptic junctions, while the synaptic contacts with dendrites were still retained (Fig. 5B). No apparent change was noticed in the postsynaptic regions at this stage, although occasional vesicles showed slight dilatation. In the granular layer of the dentate gyrus of PIMT-deficient mice, vacuolar degeneration and cytoplasmic swelling were observed in the granule cells, particularly at the axon hillock (Fig. 5C,D). These cytoplasmic changes were more prominent in the granule cells localizing closer to the subgranular zone. The vacuoles, ranging from about 90 nm to 4  $\mu$ m in diameter, were found solitarily or in clusters within the cytoplasm of PIMT-deficient mice (Fig. 5D), but not in wild-type mice (Fig. 5C). Some Golgi complexes were slightly dilated, implying that some

vacuolar changes were derived from this organelle. No necrotic neurons were observed in the granular layer. Throughout the CA3 region and the dentate gyrus of PIMT-deficient mice, astrocytes showed marked swelling from their cell bodies to the processes surrounding blood vessels, revealed by an anti-GFAP staining (data not shown). No accumulation of extracellular fluid was found in the parenchyma.

### Cognitive Deterioration in PIMT-Deficient Mice

Since the mossy fiber synapse of PIMT-deficient mice did not produce LTP, we next evaluated behavioral and cognitive abilities of 5–6-week-old PIMT-deficient mice. First, locomotor activities were recorded in a doughnut-shaped apparatus for 30 min. No significant differences in all parameters among PIMT+/+, PIMT+/-, and PIMT-/- mice were recorded: number of horizontal movement actions (ANOVA:  $F(2,31) = 0.78$ ,  $P = 0.47$ ), turning actions ( $F(2,31) = 1.64$ ,  $P = 0.21$ ), rearing actions ( $F(2,31) = 0.68$ ,  $P = 0.51$ ), total movement time ( $F(2,31) = 0.04$ ,  $P = 0.96$ ), total movement distance ( $F(2,31) = 0.15$ ,  $P = 0.86$ ), and average speed ( $F(2,31) = 0.20$ ,  $P = 0.82$ ).

The Morris water maze test was performed to assess spatial learning and memory. During habituation, mice swam randomly around the pool, showing no preference for a particular quadrant. On day 0, mice were placed in the pool with a visible platform over the water surface. Latencies to get onto the platform showed no difference among groups on day 0 (ANOVA:  $F(2,32) = 1.26$ ,  $P = 0.30$ ) (Fig. 6A). On days 1–5, the platform was hidden below the water surface, and mice performed the place learning of the platform. Escape latencies of control mice were gradually shortened and became stable by day 3. PIMT-deficient mice showed a significantly poorer performance in spatial memory acquisition (two-way ANOVA:  $F(2,120) = 16.3$ ,  $P < 0.001$ ; Tukey's test:  $Q(3,120) = 5.79$ ,  $P < 0.01$  between PIMT+/+ and PIMT-/- mice) (Fig. 6A,B). In the probe test on day 6, mice were allowed to swim freely in the pool with no platform for 90 s in order to investigate spatial bias in place learning. Although PIMT+/+ and PIMT+/- mice displayed a preference for quadrant SW where the platform had been located throughout the test, PIMT-deficient mice showed no preference, assessed by the time spent in each quadrant (Fig. 6C).

A spontaneous alternation test was conducted as another spatial-learning task (Fig. 7A). A mouse was placed in the Y-shaped maze, and behavior was observed for 8 min. PIMT+/+, PIMT+/-, and PIMT-/- mice displayed no preference for a particular arm and showed a significant alternation ratio. Thus, in contrast to the water maze test, PIMT-/- mice normally accomplished this spatial-learning task.

The step-through test, a contextual and nonspatial task, was employed to evaluate passive avoidance performance in PIMT-deficient mice (Fig. 7B). On day 1, a mouse placed in the lighted compartment showed strong preference for the dark chamber and stepped into the dark chamber within 100 s to receive an electric foot shock. The latencies to enter the dark cell showed no difference among groups (ANOVA:  $F(2,35) = 0.32$ ,  $P = 0.73$ ). Although the same procedure was performed on day

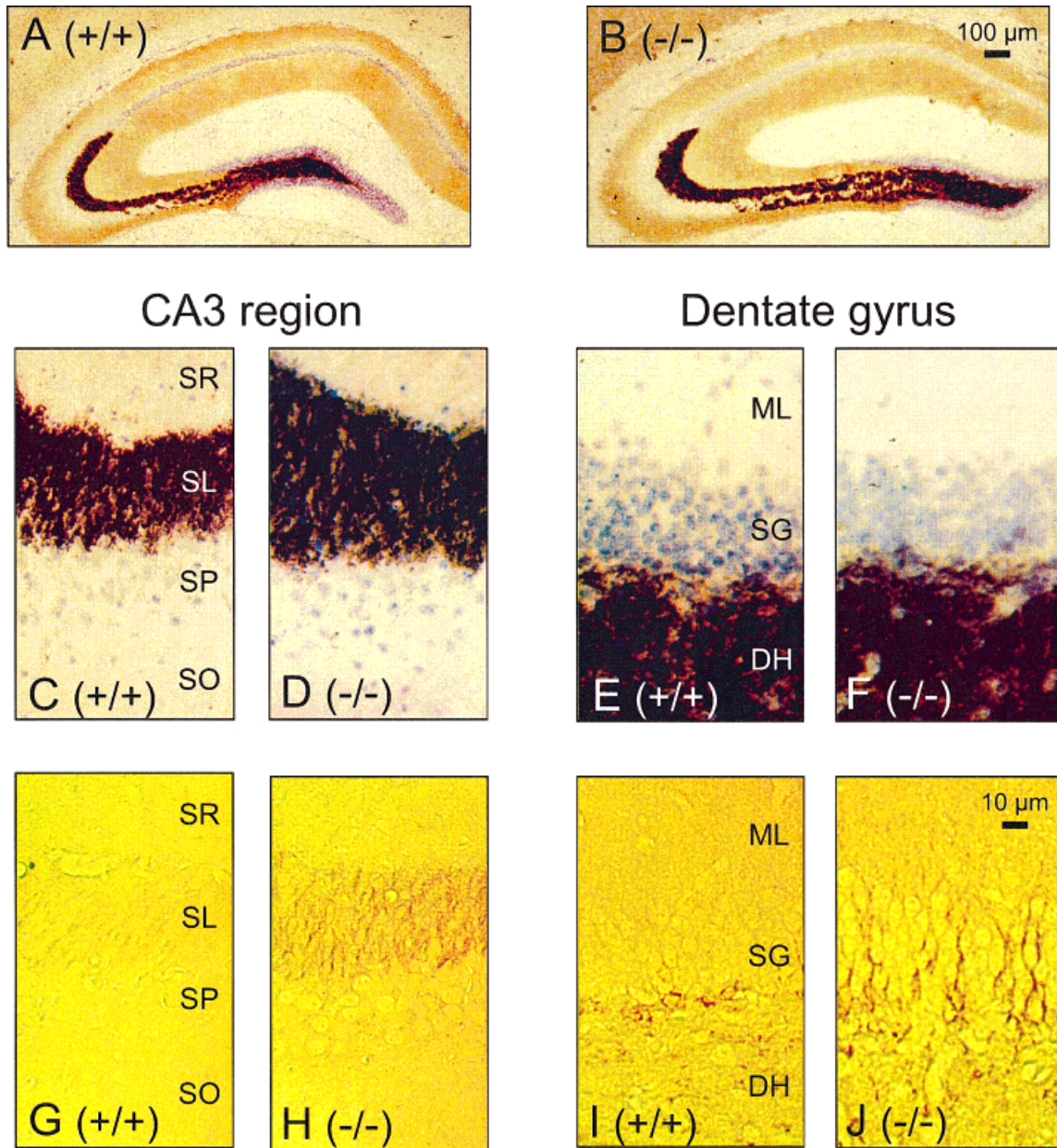


**FIGURE 4.** Light phase images of hippocampal formation (A, B), CA3 region (C, D, G, H), or dentate gyrus (E, F, I, J) of coronal brain sections stained with Timm method and cresyl violet (A–F) or immunostained with anti-PSA-NCAM antibody (G–J) in PIMT+/+ (A, C, E, G, I) or PIMT–/– (B, D, F, H, J) mouse. Timm staining studies revealed no aberration in PIMT–/– mice. Immunoreactivities for PSA-NCAM were quite high throughout the stratum lucidum of the

knockout mouse as compared to that in the wild mouse. Process-like structures that were PSA-NCAM-positive perforated perpendicularly through the stratum granulosum of PIMT–/– mice. SR, stratum radiatum; SL, stratum lucidum; SP, stratum pyramidale; SO, stratum oriens; ML, dentate molecular layer; SG, stratum granulosum; DH, dentate hilus.

2, 11 of 13 PIMT+/+ mice and 11 out of 14 PIMT+/- mice did not enter the dark compartment and halted in the bright room during the observation period (300 s). However, all of 11 PIMT–/– mice got into the dark chamber. Accordingly, the average latency to enter the dark compartment was significantly shorter in PIMT-deficient mice than that in the control mice (ANOVA:  $F(2,35) = 19.5, P < 0.001$ ; Tukey’s test:  $Q(3,35) = 7.80, P < 0.01$ ).

Finally, we tested the mice in an elevated-plus maze to examine their anxiety-related behavior (Pellow et al., 1985). PIMT+/+ and PIMT+/- mice spent a longer time in the closed arms than in the open arms. In PIMT–/– mice, however, a percentage of time spent on the open arms increased almost close to a chance level (Fig. 7C). This result indicated that PIMT-deficient mice appeared to feel less anxiety under the experimental conditions than the control animals.

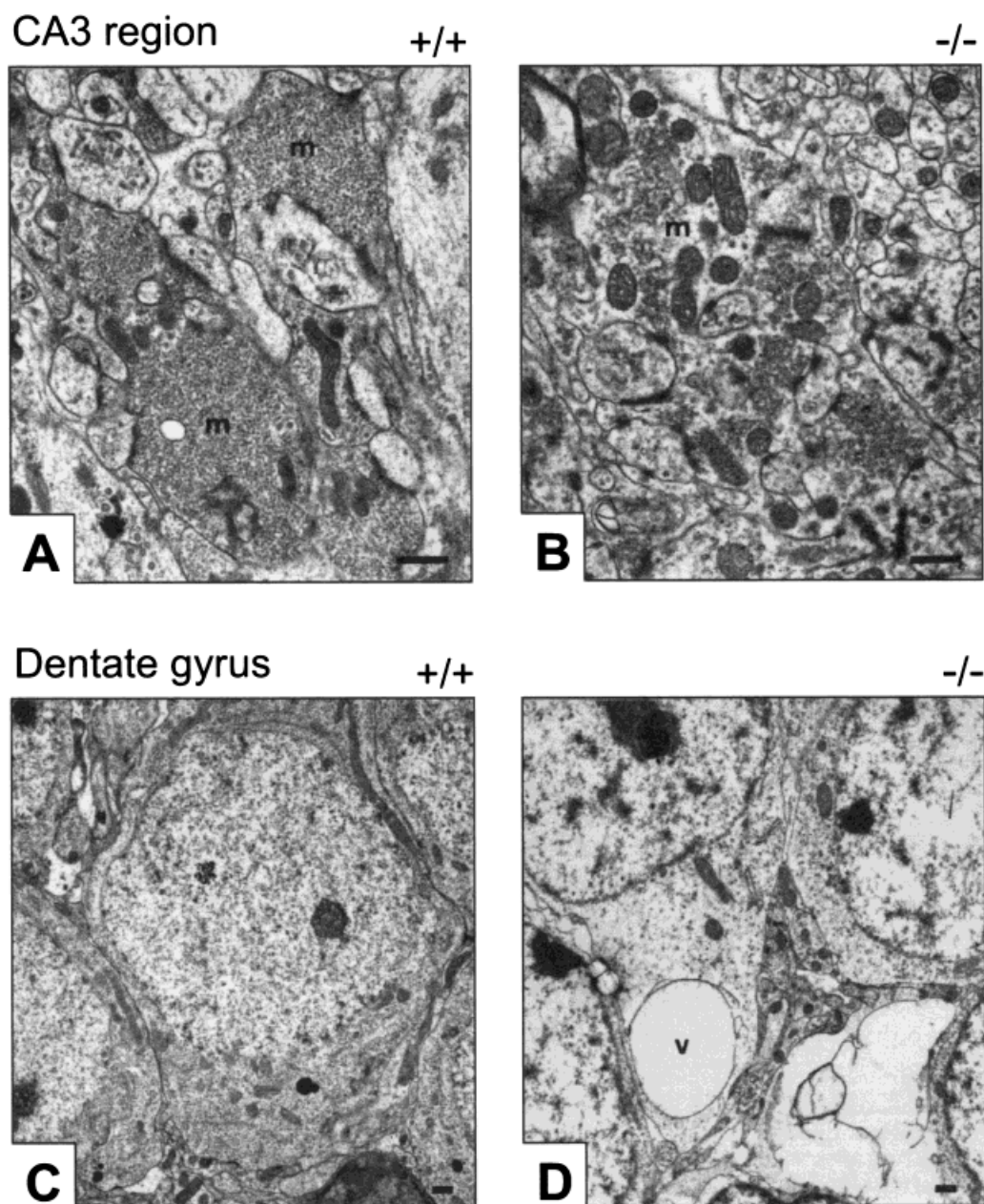


**FIGURE 5.** Electron microscopic images of hippocampal formation from PIMT+/+ and PIMT-/- mice. Mossy fibers were in stratum lucidum of PIMT+/+ (A) and PIMT-/- mouse (B). Synaptic vesicles in mossy fiber terminals (m) of knockout mouse showed aggregation and a reduction in number. Also shown is stratum granu-

losum in dentate gyrus of PIMT+/+ (C) and PIMT-/- mouse (D). Vacuolar degeneration (v) and cytoplasmic swelling are seen in granule cells, particularly at the axon hillock, of PIMT-/- mouse. Scale bars, 500 nm.

## DISCUSSION

We have shown aberrant neurotransmission in mossy fiber-CA3 synapses and histological abnormalities in the axon terminals as well as in the axon hillocks of dentate granule cells in the hippocampus of PIMT-deficient mice. Furthermore, cognitive deficits and emotional alternations were apparent in PIMT-deficient mice. These aberrations were likely associated with the onset of epileptic seizures.

### Characteristic Mossy Fiber Degeneration in PIMT-Deficient Mice

The mossy fiber synapses of PIMT-deficient mice displayed hyperexcitability after stimulation of the dentate gyrus. Additionally, immunoreactivity for PSA-NCAM in the stratum lucidum was augmented in PIMT-deficient mice. PSA-NCAM is abundantly expressed in neurons with a high level of synaptic plasticity, probably related to the potential to change their morphology (Seki and Arai, 1993; Theodosis et al., 1994; Muller et al., 1996; Allan and



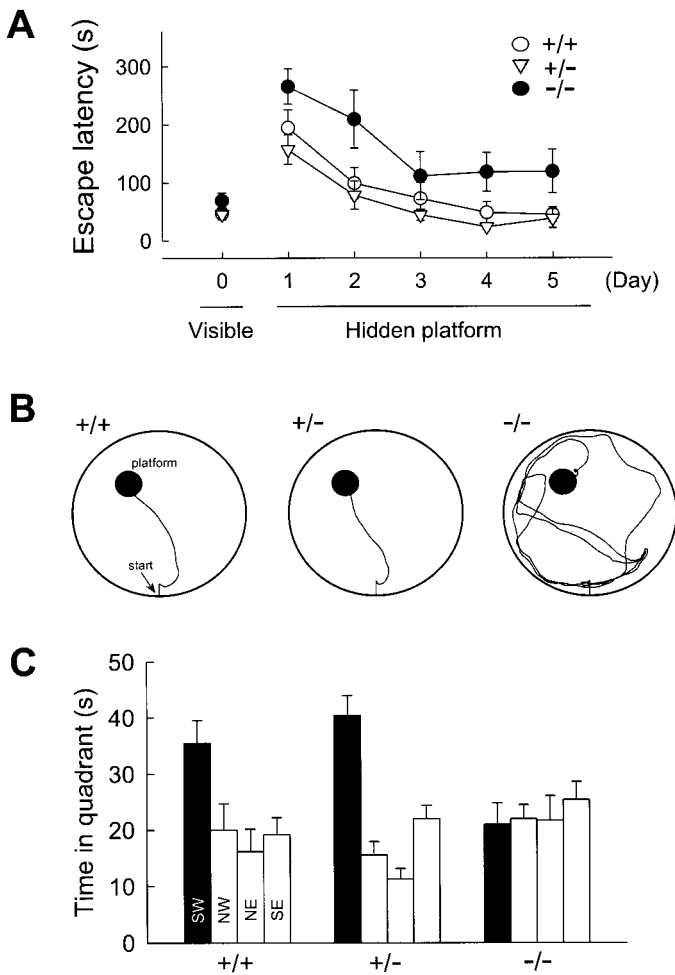
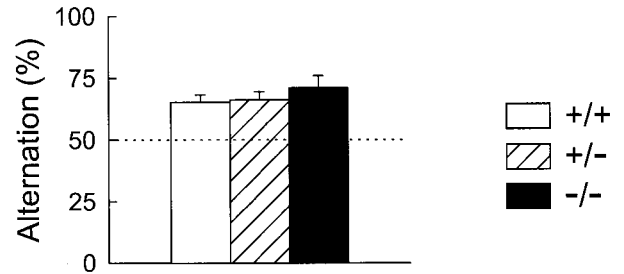


**FIGURE 6.** Behavioral performance of 5-week-old mouse in Morris water maze task. **A:** Escape latencies to get onto platform that was visible on day 0 and was hidden in training session on days 1–5 were monitored in PIMT+/+ (open circles), PIMT+/- (open triangles), and PIMT-/- mice (solid circles). **B:** Typical swimming paths taken by PIMT+/+ (left), PIMT+/- (center), and PIMT-/- mice (right) on day 5 in training session. Solid circles indicate location of platform. **C:** Posttraining retention task of water maze (probe test) was conducted on day 6. The ordinate indicates total duration that the mouse swam in quadrant SW, NW, NE, or SE. Quadrant SW is the area where the platform was located throughout the training session. Performance of PIMT-/- mouse in the water maze test was severely impaired both in the training session and in the probe trial. Data represent mean  $\pm$  SEM of 8–14 cases.

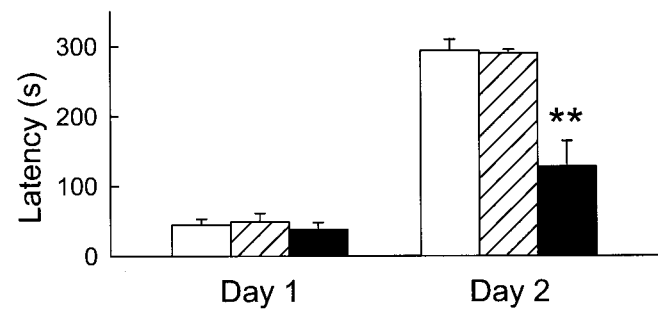
Greer, 1998). These findings are consistent with the hyperexcitable synapses of mossy fibers in PIMT-deficient mice. Although the molecular mechanisms underlying the hyperexcitability remain to be defined, our pharmacological data indicate that muscimol completely reduced the prolonged duration of fEPSP, suggesting that functional GABA receptors are not adequately stimulated in PIMT-deficient mice. Because GAD-65/67 or GABA immunoreactivity was unaffected in PIMT-deficient mice, the decrease in GABA release rather than GABA synthesis may be a causal factor of the hyperexcitability in CA3 pyramidal neurons. As for a putative mechanism of the hyperexcitable neurotransmission in mossy fi-

ber-CA3 neurons, the following evidence suggests presynaptic aberration in PIMT-deficient mice. First, LTP was suppressed selectively at mossy fiber-CA3 synapses in PIMT-deficient mice, where LTP was induced purely through presynaptic and NMDA receptor-independent mechanisms (Nicoll and Malenka, 1995). Sec-

**A Spontaneous alternation behavior test**



**B Step-through test**



**C Elevated plus maze test**

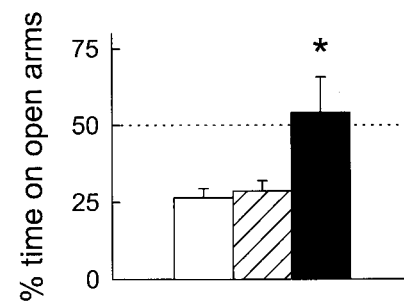


**FIGURE 7.** Behavioral performance in spontaneous alternation behavior test (A), step-through test (B), or elevated-plus test (C) of 5–6-week-old PIMT+/+ (open columns), PIMT+/- (hatched columns), and PIMT-/- (solid columns) mouse. **A:** Spontaneous alternation behavior in Y-shaped maze was observed for 8 min. Dashed line indicates chance level of alternation ratio. All groups showed significant alternation ratios. **B:** Ordinate indicates latencies to enter the dark chamber in the learning trial (Day 1) or the testing trial (Day 2). The knockout mouse showed poor performance on day 2. \*\* $P < 0.01$  vs. the wild mouse: Tukey’s test following ANOVA. **C:** Ordinate indicates ratio of total duration that the mouse stayed on open arms for the observation period of 3 min. Dashed line indicates blind level. PIMT-/- mouse spent more time in the open arms than did the other groups. Each bar represents means  $\pm$  SEM of 8–14 cases. \* $P < 0.05$  vs. the wild mouse: Turkey’s test following ANOVA.

ondly, lack of paired-pulse facilitation strongly implicates presynaptic dysfunction (Zucker, 1989). Thirdly, the electron microscopic analysis of the hippocampi of PIMT-deficient mice revealed abnormal distribution of synaptic vesicles in the mossy fiber terminals, but no histological aberration was observed in postsynaptic sites. Taken together, postsynaptic alterations were virtually undetected in our physiological and morphological studies. Rather, on the basis of deviant immunoreactivity for PSA-NCAM, vacuolar degeneration, and cytoplasmic swelling in the stratum granulare, we consider that the degeneration of dentate granule cells descends anterogradely to the mossy fiber terminals and thereby changes mossy fiber-CA3 synaptic transmission.

Because there was little variability in the onset of epileptic seizures in the mice, we were not able to compare epileptic PIMT-deficient mice with asymptomatic PIMT-deficient mice as age-matched controls. However, because aberrant neurotransmission was not observed in the mossy fiber-CA3 synapse in the 3-week-old seizure-free mice, it is our impression that the electrophysiological and histological aberrations in the mossy fiber system of PIMT-deficient mice are associated with the onset of epileptic seizures. Although the causal relation between mossy fiber abnormality and epilepsy has not been resolved, it is possible that the hyperactive inputs via aberrant mossy fibers evoke ictal discharges in CA3 pyramidal cells, which consequently develop into the generalized seizure, because the CA3 pyramidal cells, the most excitable neurons among the hippocampal principal neurons, can serve as a generator of epileptiform firings (Miles et al., 1984; Scharfman, 1994). Therefore, the CA3 region, particularly the mossy fibers, may be a primary focus of epilepsy in PIMT-deficient mice.

### Collapsed Plasticity of PIMT-Deficient Mice

Mossy fiber-CA3 LTP did not occur in PIMT-deficient mice, while Schaffer collateral-CA1 LTP was intact. As PIMT was ubiquitously distributed, the reason for the selective loss of CA3 LTP remains uncertain. One possible explanation is that epileptic activity results in the loss of CA3 LTP. Because epileptiform activities induce long-lasting enhancement of synaptic strength similar to LTP (Ben-Ari and Represa, 1990), it is plausible that LTP in PIMT-deficient mice had been saturated by the hyperexcitability of mossy fiber synapses (Piredda et al., 1986; Moore et al., 1993; Stewart and Reid, 1993; Stewart et al., 1994). Indeed, the enlarged baseline fEPSP in PIMT-deficient mice suggests the preexistence of LTP. Moreover, paired-pulse plasticity is known to alter in hippocampi of epileptic animals (Lopes da Silva et al., 1994; Leung et al., 1994). PIMT<sup>-/-</sup> mossy fiber synapses exhibited paired-pulse depression rather than the paired-pulse facilitation. This may also be a consequence of epileptiform activity. Synaptic vesicles of the mossy fiber terminals were sparsely distributed. This can also be explained by the observation that the vesicles were excessively consumed by hyperactive discharges of mossy fibers. The insufficiency of available synaptic vesicles may thus account for the alteration in mossy fiber plasticity. However, the depletion of synaptic vesicles in the mossy fiber terminals cannot account for the aberrant field potential in PIMT-deficient mice. The causal relation for the col-

lapse of synaptic plasticity between the depleted vesicles and the hyperactivity remains to be elucidated.

Another explanation for the selective loss of CA3 LTP is that the decrease in vesicle density is due to a cytoskeletal malfunction. If the vesicle-holding cytoskeleton loses normal function, the vesicle density in presynaptic buttons will be markedly reduced. Interestingly, previous studies showed that aspartate residues of tubulin (Najbauer et al., 1996) and synapsin I (Paranandi and Aswad, 1995) are vulnerable to spontaneous isomerization. Because such isomerized residues in vesicle-associated protein are not repaired in PIMT-deficient mice, their vesicle-holding capacity might deteriorate. From this point of view, another possibility is raised. Because the mechanisms of mossy fiber-CA3 LTP and Schaffer collateral-CA1 LTP are quite distinct (Nicoll and Malenka, 1995), CA3 LTP is selectively impaired when certain molecules involved specifically in CA3 LTP are degenerated. Alternatively, proteins that require PIMT for repairing their aspartate isomerization may mediate CA3 LTP induction. To clarify these possibilities, further biochemical analysis of L-isoaspartate accumulation in the putative substrate proteins, including cytoskeleton constituents or synaptic devices in PIMT-deficient mice, is now underway.

### Cognitive Deterioration in PIMT-Deficient Mice

Among the hippocampal subregions, the CA3 region is particularly important for high-order functioning of the central nervous system, such as the store of episodic information and the recall of a memory, i.e., learning and memory (Treves and Rolls, 1994). As far as the animals produced by gene targeting are concerned, two lines of knockout mice have exhibited a selective loss of mossy fiber-CA3 LTP: Rab3A-deficient mice (Castillo et al., 1997) and adenylyl cyclase I-deficient mouse (Villacres et al., 1998). However, the cognitive ability of these mice was not addressed in the above studies. In the present study, we made extensive investigations of intellectual and emotional performance of PIMT-deficient mice. To our knowledge, this report is the first implication for a correlation between the mossy fiber system and cognitive processing. On the basis of the fact that water maze performance depends predominantly on reference memory while spontaneous alternation behavior depends only on working memory (Olton and Papas, 1979; Cain and Saucier, 1996; Hodges, 1996), our results suggest that mossy fibers are required for the processing of reference memory but not for working memory. Johnson et al. (1977) reported that alternation behavior is disrupted by hippocampal lesions. Therefore, processing of short-term memory in the hippocampus may be mediated by other neural pathways, e.g., Schaffer collateral-CA1 synapses, the perforant path-dentate gyrus, and associational/commissural fibers. The hypothesis that mossy fibers serve as a processing apparatus of long-term memory is further supported by the impaired performance of PIMT-deficient mice in the step-through test, because this result also indicates that the mice could not maintain their aversive memory, i.e., nonspatial reference memory. Indeed, Lisman (1999) proposed that CA3 pyramidal cells that encode a given event in a given context have strong recurrent connections with the next event in the sequence, thereby building up the complete episodic memory. This proposal

is very consistent with our consideration that the mossy fiber system plays a crucial role in long-term declarative memory processing.

It is interesting to note that PIMT-deficient mice displayed less anxiety-related behavior in the elevated-plus maze. This finding is also the first implication for a role of mossy fibers in motivational and emotional modulations. However, it is possible that the anxiolytic effect might also be detected in animals which are less sensitive to the conditions of task or to the aversive environmental stimuli, i.e., water and foot shock. Therefore, further physiological and histological characterizations of other brain regions, including the amygdala as well as the hippocampus, would be required for a precise conclusion.

The accumulation of damaged proteins has been thought to play a role in the aging process (Harding et al., 1989; Stadtman, 1992; Visick and Clarke, 1995; Martin et al., 1996), and PIMT is thought to retard the aging process at the cellular as well as tissue levels. Here we suggest another role of PIMT. Even in the brain of young adult (not aged) PIMT-deficient mice, synaptic transmission is indisposed. These results suggest that PIMT dynamically modulates synaptic function. Aspartate isomerization and methylation of L-isoaspartate residues may serve as a modulator of protein activity in synaptic transmission. PIMT-deficient mice thus provide insight into unidentified functions of aspartate isomerization in both physiological and pathological aspects.

## Acknowledgments

We thank Dr. T. Seki, (Juntendo University) for generously supplying antibodies against PSA-NCAM, Dr. Y. Takahashi (Nigata University) for generously providing antiserum against NF, and Dr. A. Yamamoto (Tokyo Metropolitan Institute of Psychiatry), Dr. K. Kawamura (Keio University), Dr. H. Kawano (Tokyo Metropolitan Institute of Neuroscience), Dr. M. Ogawara and Dr. T. Shimizu (Tokyo Metropolitan Institute of Gerontology), and Dr. H. Mori (Osaka Municipal University) for their technical support and kind comments on the experiment.

## REFERENCES

- Allan DW, Greer JJ. 1998. Polysialylated NCAM expression during motor axon outgrowth and myogenesis in the fetal rat. *J Comp Neurol* 391:275–292.
- Babb TL, Kupfer WR, Pretorius JK, Crandall PH, Levesque MF. 1991. Synaptic reorganization by mossy fibers in human epileptic fascia dentata. *Neuroscience* 42:351–363.
- Ben-Ari Y, Represa A. 1990. Brief seizure episodes induce long-term potentiation and mossy fibre sprouting in the hippocampus. *Trends Neurosci* 13:312–318.
- Bliss TV, Collingridge GL. 1993. A synaptic model of memory: long-term potentiation in the hippocampus. *Nature* 361:31–39.
- Cain DP, Saucier D. 1996. The neuroscience of spatial navigation: focus on behavior yields advances. *Rev Neurosci* 7:215–231.
- Carlton SM, Hayes ES. 1990. Light microscopic and ultrastructural analysis of GABA-immunoreactive profiles in the monkey spinal cord. *J Comp Neurol* 300:62–182.
- Castillo PE, Janz R, Sudhof TC, Tzounopoulos T, Malenka RC, Nicoll RA. 1997. Rab3A is essential for mossy fibre long-term potentiation in the hippocampus. *Nature* 388:590–593.
- Clarke S. 1985. Protein carboxyl methyltransferases: two distinct classes of enzymes. *Annu Rev Biochem* 54:479–506.
- Danscher G, Zimmer J. 1978. An improved Timm sulphide silver method for light and electron microscopic localization of heavy metals in biological tissues. *Histochemistry* 55:27–40.
- Erlander MG, Tillakaratne NJK, Feldblum S, Patel N, Tobin AJ. 1991. Two genes encode distinct glutamate decarboxylases. *Neuron* 7:91–100.
- Fukuda T, Kawano H, Ohyama K, Li H-P, Takeda Y, Oohira A, Kawamura K. 1997. Immunohistochemical localization of neurocan and L1 in the formation of thalamocortical pathway of developing rats. *J Comp Neurol* 382:141–152.
- Galletti P, Ingrosso D, Manna C, Clemente G, Zappia V. 1995. Protein damage and methylation-mediated repair in the erythrocyte. *Biochem J* 306:313–325.
- Geiger T, Clarke S. 1987. Deamidation, isomerization, and racemization at asparaginy and aspartyl residues in peptides. Succinimide-linked reactions that contribute to protein degradation. *J Biol Chem* 262:785–794.
- Harding JJ, Beswick HT, Ajiboye R, Huby R, Blakytyn R, Rixon KC. 1989. Non-enzymic post-translational modification of proteins in aging. A review. *Mech Aging Dev* 50:7–16.
- Hodges H. 1996. Maze procedures: the radial-arm and water maze compared. *Cogn Brain Res* 3:167–181.
- Ikegaya Y. 1999. Abnormal targeting of developing hippocampal mossy fibers following epileptiform activities via L-type  $Ca^{2+}$  channel activation in vitro. *J Neurosci* 19:802–812.
- Ikegaya Y, Nishiyama N, Matsuki N. 2000. L-type  $Ca^{2+}$  channel blocker inhibits mossy fiber sprouting and cognitive deficits following pilocarpine seizures in immature mice. *Neuroscience* 98:647–659.
- Izquierdo I, Medina JH. 1995. Correlation between the pharmacology of long-term potentiation and the pharmacology of memory. *Neurobiol Learn Mem* 63:19–32.
- Johnson BA, Langmack EL, Aswad DW. 1987. Partial repair of deamidation-damaged calmodulin by protein carboxyl methyltransferase. *J Biol Chem* 262:12283–12287.
- Johnson BA, Ngo SQ, Aswad DW. 1991. Widespread phylogenetic distribution of a protein methyltransferase that modifies L-isoaspartyl residues. *Biochem Int* 24:841–847.
- Johnson CT, Olton DS, Gage FH, Jenko PG. 1977. Damage to hippocampus and hippocampal connections: effects of DRL and spontaneous alternation. *J Comp Physiol Psychol* 91:508–522.
- Kim E, Lowenson JD, MacLaren DC, Clarke S, Young SG. 1997. Deficiency of a protein-repair enzyme results in the accumulation of altered proteins, retardation of growth, and fatal seizures in mice. *Proc Natl Acad Sci USA* 94:6132–6137.
- Ladino CA, O'Connor CM. 1992. Methylation of atypical protein aspartyl residues during the stress response of HeLa cells. *J Cell Physiol* 153:297–304.
- Leung LS, Zhao D, Shen B. 1994. Long-lasting effects of partial hippocampal kindling on hippocampal physiology and function. *Hippocampus* 4:696–704.
- Lindquist JA, McFadden PN. 1994. Automethylation of protein (D-aspartyl/L-isoaspartyl) carboxyl methyltransferase, a response to enzyme aging. *J Protein Chem* 13:23–30.
- Lisman JE. 1999. Relating hippocampal circuitry to function: recall of memory sequences by reciprocal dentate-CA3 interactions. *Neuron* 22:233–242.
- Lopes da Silva FH, Pijn JP, Wadman WJ. 1994. Dynamics of local neuronal networks: control parameters and state bifurcations in epileptogenesis. *Prog Brain Res* 102:359–370.
- Martin GM, Austad SN, Johnson TE. 1996. Genetic analysis of aging: role of oxidative damage and environmental stresses. *Nat Genet* 13:25–34.

- Martinez JL Jr, Derrick BE. 1996. Long-term potentiation and learning. *Annu Rev Psychol* 47:173–203.
- McFadden PN, Clarke S. 1987. Conversion of isoaspartyl peptides to normal peptides: implications for the cellular repair of damaged proteins. *Proc Natl Acad Sci USA* 84:2595–2599.
- Mercken M, Luebke U, Vandermeeren M, Gheuens J, Oestreicher AB. 1992. Immunocytochemical detection of the growth-associated protein B-50 by newly characterized monoclonal antibodies in human brain and muscle. *J Neurobiol* 23:309–321.
- Miles R, Wong RK, Traub RD. 1984. Synchronized afterdischarges in the hippocampus: contribution of local synaptic interactions. *Neuroscience* 12:1179–1189.
- Moore SD, Barr DS, Wilson WA. 1993. Seizure-like activity disrupts LTP in vitro. *Neurosci Lett* 163:117–119.
- Morris R. 1984. Developments of a water-maze procedure for studying spatial learning in the rat. *J Neurosci Methods* 11:47–60.
- Muller D, Wang C, Skibo G, Toni N, Cremer H, Calaora V, Rougon G, Kiss JZ. 1996. PSA-NCAM is required for activity-induced synaptic plasticity. *Neuron* 17:413–422.
- Najbauer J, Orpiszewski J, Aswad DW. 1996. Molecular aging of tubulin: accumulation of isoaspartyl sites in vitro and in vivo. *Biochemistry* 35:5183–5190.
- Nicoll RA, Malenka RC. 1995. Contrasting properties of two forms of long-term potentiation in the hippocampus. *Nature* 377:115–118.
- Olton DS, Papas BC. 1979. Spatial memory and hippocampal function. *Neuropsychologia* 17:669–682.
- Paranandi MV, Aswad DW. 1995. Spontaneous alterations in the covalent structure of synapsin I during in vitro aging. *Biochem Biophys Res Commun* 212:442–448.
- Pellow S, Chopin P, File SE, Briley M. 1985. Validation of open:closed arm entries in an elevated plus-maze as a measure of anxiety in the rat. *J Neurosci Methods* 14:149–167.
- Piredda S, Yonekawa W, Whittingham TS, Kupferberg HJ. 1986. Enhanced bursting activity in the CA3 region of the mouse hippocampal slice without long-term potentiation in the dentate gyrus after systemic pentylenetetrazole kindling. *Exp Neurol* 94:659–669.
- Scharfman HE. 1994. Synchronization of area CA3 hippocampal pyramidal cells and non-granule cells of the dentate gyrus in bicuculline-treated rat hippocampal slices. *Neuroscience* 59:245–257.
- Schwartzkroin PA. 1994. Role of the hippocampus in epilepsy. *Hippocampus* 4:239–242.
- Seki T, Arai Y. 1991. Expression of highly polysialylated NCAM in the neocortex and piriform cortex of the developing and the adult rat. *Anat Embryol (Berl)* 184:395–401.
- Seki T, Arai Y. 1993. Highly polysialylated neural cell adhesion molecule (NCAM-H) is expressed by newly generated granule cells in the dentate gyrus of the adult rat. *J Neurosci* 13:2351–2358.
- Stadtman ER. 1992. Protein oxidation and aging. *Science* 257:1220–1224.
- Stephenson RC, Clarke S. 1989. Succinimide formation from aspartyl and asparaginyl peptides as a model for the spontaneous degradation of proteins. *J Biol Chem* 264:6164–6170.
- Stewart C, Reid I. 1993. Electroconvulsive stimulation and synaptic plasticity in the rat. *Brain Res* 620:139–141.
- Stewart C, Jeffery K, Reid I. 1994. LTP-like synaptic efficacy changes following electroconvulsive stimulation. *Neuroreport* 5:1041–1044.
- Sutula T, He XX, Cavazos J, Scott G. 1988. Synaptic reorganization in the hippocampus induced by abnormal functional activity. *Science* 239:1147–1150.
- Tauck DL, Nadler JV. 1985. Evidence of functional mossy fiber sprouting in hippocampal formation of kainic acid-treated rats. *J Neurosci* 5:1016–1022.
- Theodosis DT, Bonfanti L, Olive S, Rougon G, Poulain DA. 1994. Adhesion molecules and structural plasticity of the adult hypothalamo-neurohypophysial system. *Psychoneuroendocrinology* 19:455–462.
- Treves A, Rolls ET. 1994. Computational analysis of the role of the hippocampus in memory. *Hippocampus* 4:374–391.
- Van der Zee CE, Rashid K, Le K, Moore KA, Stanis J, Diamond J, Racine RJ, Fahnstock M. 1995. Intraventricular administration of antibodies to nerve growth factor retards kindling and blocks mossy fiber sprouting in adult rats. *J Neurosci* 15:5316–5323.
- Villacres EC, Wong ST, Chavkin C, Storm DR. 1998. Type I adenylyl cyclase mutant mice have impaired mossy fiber long-term potentiation. *J Neurosci* 18:3186–3194.
- Visick JE, Clarke S. 1995. Repair, refold, recycle: how bacteria can deal with spontaneous and environmental damage to proteins. *Mol Microbiol* 16:835–845.
- Yamamoto A, Takagi H, Kitamura D, Tatsuoka H, Nakano H, Kawano H, Kuroyanagi H, Yahagi Y, Kobayashi S, Koizumi K, Sakai T, Saito K, Chiba T, Kawamura K, Suzuki K, Watanabe T, Mori H, Shirasawa T. 1998. Deficiency in protein L-isoaspartyl methyltransferase results in a fatal progressive epilepsy. *J Neurosci* 18:2063–2074.
- Zucker RS. 1989. Short-term synaptic plasticity. *Annu Rev Neurosci* 12:13–31.